

Characteristics measurement of plastic scintillators and performance evaluation of cosmic ray measurement for the ALPAQUITA experiment

Mizuno Atsushi for the ALPACA collaboration^a

^a*Institute for Cosmic Ray Research, University of Tokyo
Kashiwanoha, Kashiwa, Chiba 277-8582, Japan*

E-mail: mizuno@icrr.u-tokyo.ac.jp

The ALPACA experiment is an extensive air shower array located in Bolivia, South America, consisting of 401 detectors each with an effective area of 1 m^2 , covering a total surface area of $83,000\text{ m}^2$. In addition, an underground muon detector system is installed, comprising detectors placed 2 meters below ground level with a total sensitive area of $3,600\text{ m}^2$.

Measurements of the scintillator characteristics were performed under conditions closely replicating the actual setup used in the ALPAQUITA experiment. Specifically, we measured the scintillation light yield (charge), light collection time, and signal rise time, as well as their position dependence, using the same type of scintillators deployed in ALPAQUITA.

The results showed that the light yield near the corners was approximately 20% lower than at the center. In terms of signal timing, a delay of about 0.2 ns was observed for particles entering near the corners compared to those entering near the center.

As a prototype array for the ALPACA experiment, the ALPAQUITA experiment—with one-quarter the areal coverage—commenced data acquisition in April 2023. In the ALPAQUITA surface array, data are recorded under trigger conditions categorized as any1 through any4, corresponding to the number of detectors registering coincident particle hits. The observed trigger rates were 78,000 Hz for any1, 4,800 Hz for any2, 600 Hz for any3, and 300 Hz for any4. Among these, the true rate for any2, corrected for accidental coincidences, was determined to be 1,400 Hz.

In addition, we compared several reconstructed shower parameters between the Monte Carlo simulations and the ALPAQUITA experimental data. This included the even-odd opening angle, which serves as a proxy for the angular resolution of the detector system. The even-odd opening angle measured in the ALPAQUITA surface array was 1.95° , closely matching the value of 1.76° obtained from the simulation. These results demonstrate that the Monte Carlo simulations incorporating the measured scintillator characteristics accurately reproduce the performance of the ALPACA and ALPAQUITA experiments. This, in turn, indicates that the energy spectra of gamma-ray sources observed with ALPACA and ALPAQUITA can be estimated with high precision.

39th International Cosmic Ray Conference (ICRC2025)
15–24 July 2025
Geneva, Switzerland



1. Introduction

In 2019, the Tibet AS γ experiment reported the detection of ~ 450 TeV gamma rays from the Crab Nebula [1], marking the first observation of gamma rays exceeding 100 TeV worldwide. Following this discovery, numerous observations of gamma rays above 100 TeV have been conducted in the northern sky. However, to date, no experiment exists that can measure gamma rays in the 100 TeV energy range with good sensitivity in the southern sky. The southern sky includes the Galactic Center and Galactic Plane regions, which are particularly important targets for the search for PeVatrons because of their high matter density and intense star-forming activity. As the first southern sub-PeV observatory, a new airshower array experiment, the Andes Large area PArticle detector for Cosmic ray physics and Astronomy (ALPACA), is under construction near the Chacaltaya mountain in Bolivia at an altitude of 4,740 m [2] [3].

In this study, we performed a detailed characterization of the plastic scintillators employed in the ALPAQUITA experiment. Measurements were conducted under conditions closely resembling the actual experimental setup used in ALPAQUITA. Specifically, we evaluated the scintillation light yield (measured as charge), light collection time, signal rise time, and their position dependencies using the same type of scintillators implemented in the experiment.

2. ALPAQUITA Array

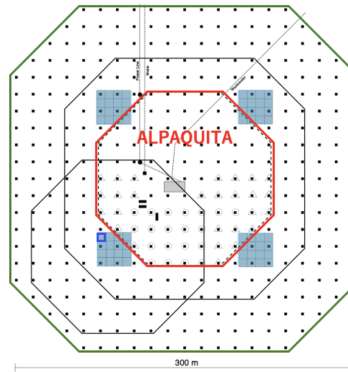


Figure 1: Overview of the ALPACA experiment. Each black dot represents an individual scintillation detector. The light blue region indicates the underground muon detector. The area enclosed in red corresponds to the ALPAQUITA array.

The detector layout of the ALPACA experiment is shown in Figure 1. Each black dot represents a surface detector, and the light blue region indicates the underground muon detector. As shown in Figure 2, the surface array consists of 401 plastic scintillators, each with a detection area of 1 m^2 , arranged at 15 m intervals, covering a total area of $83,000 \text{ m}^2$. Scintillation light is diffusely reflected within the detector housing and collected by a photomultiplier tube (PMT) mounted beneath each detector. The magnitude of the detected signal provides information on the size of the air shower and is used to estimate the energy of the primary cosmic ray. In addition, the timing information of the detected signals is used to reconstruct the arrival direction.

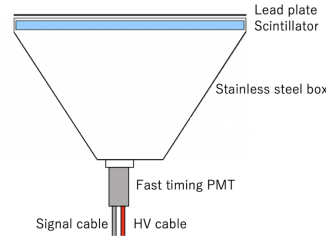


Figure 2: Design of an individual scintillation detector comprising the air shower array of the ALPACA experiment. A plastic scintillator with an area of $1m^2$ is enclosed in a stainless-steel housing, with a 5mm thick lead plate placed on top.

3. Characteristics measurement of plastic scintillators

3.1 Measurement

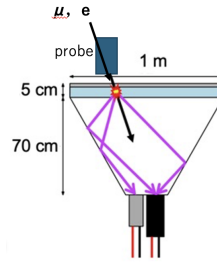


Figure 3: Design of an individual scintillation detector comprising the air shower array of the ALPACA experiment. A $1m^2$ plastic scintillator is enclosed in a stainless steel housing, with a 5 mm-thick lead plate placed on top. A probe detector providing external triggers was placed on top of the detector to take calibration data described in this paper.

The characteristics of the scintillator, photomultiplier tube (PMT), and housing box used in the ALPAQUITA experiment were measured at lab using a probe detector. The probe detector (shown at the top of Figure 3) consists of a 2-inch PMT and a 2-inch diameter scintillator placed above a $1m^2$ detector, and is used as an external trigger device. By triggering with the probe detector, the passage location of cosmic rays through the main detector was specified. Measurements of the scintillation light yield, light collection time, and signal rise time of the scintillator were performed. To evaluate position dependence, the probe detector was moved to eight different positions, as illustrated in Figure 4. The applied high voltage was adjusted so that the ADC peak value would be approximately 120 pC, corresponding to the actual operating conditions in the ALPACA experiment.

3.2 Result

Figure 3 shows an example of charge distribution after subtracting the pedestal value when the probe detector was placed at the center of the detector (position 1 in Fig.1). In the range of 10 to 50 pC, the distribution was fitted with a Landau function convoluted with a Gaussian function

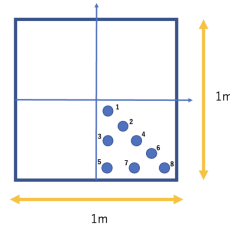


Figure 4: Locations of the probe detector placed on the detector

(to account for the detector resolution), as shown by the red curve. The peak value in this range was defined as the MPV (Most Probable Value) of the charge distribution. Figure 4 shows another example when the probe detector was placed at the corner of the detector (position 8 in Fig.1).

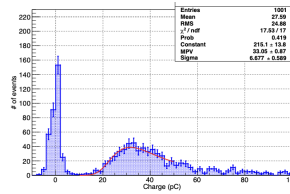


Figure 5: A charge distribution of an ALPACA detector when the probe detector was placed at the position 1 of Figure 1. The horizontal axis represents the charge, and the vertical axis represents the number of events.

A comparison of MPV values between position 1 (near the center) and position 8 (near the corner) showed a difference of more than 20%.

The timing measurement results are presented. The horizontal axis represents the relative time difference between the signals from the target scintillator and the probe detector, measured in nanoseconds. The vertical axis indicates the number of events per bin. The red curve shows the result of a Gaussian fit to the distribution, and the mean of the fitted Gaussian was taken as the signal delay.

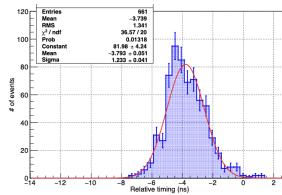


Figure 6: Timing distribution of an ALPACA detector relative to the probe signal when the probe detector was placed at the position 1. The horizontal axis represents the charge, and the vertical axis represents the number of events.

The signal is delayed more at position 8 (near the corner). The t.t.s. is larger at position 8 as well.

4. Simulation condition

4.1 Simulation condition

We performed air shower simulations in the atmosphere to obtain the position, arrival time, energy, momentum, and particle species of individual secondary particles at the altitude corresponding to the ALPAQUITA site. The simulation conditions used in this study are summarized in Table 1. The air shower core positions were randomly distributed within a circular area of radius 300 m centered on the ALPAQUITA array. For the cosmic-ray spectrum, we adopted a composition model [4] in which the elemental abundances are adjusted to reproduce the results of direct observations by balloon- and satellite-borne experiments, as illustrated in Fig. 1. Simulation Set 1, with primary energies ranging from 280 MeV to 10 TeV, was designed to cover the low-energy regime, while Simulation Set 2, spanning from 300 GeV to 10 PeV, was intended to increase the statistics in the high-energy range. In both cases, 10^9 primary cosmic ray events were simulated.

The position dependence of the scintillation light yield (charge), signal delay, and transit time spread (T.T.S.) of the scintillators actually used in the ALPAQUITA experiment was incorporated into the Monte Carlo simulation. Based on these implementations, we compared the simulation results with observational data and evaluated the detector performance.

The development of air showers induced by cosmic rays was simulated using CORSIKA version 7.6400 [5], while the detector response after particle entry was modeled using Geant4 version 10.04.p02 [6].

Simulation condition	Value
Energy region	1. $280 \text{ MeV} \leq E < 10 \text{ TeV}$ 2. $300 \text{ GeV} \leq E < 10 \text{ PeV}$
# of events	1. 10^9 events 2. 10^9 events

Table 1: Simulation conditions.

4.2 Results

A comparison between the experimental results and Monte Carlo simulations shows good agreement for any2 through any4. However, for any1, the Monte Carlo counting rate is approximately 30% lower than the experimental result.

Next, we introduce the quantity called the even-odd opening angle. As illustrated in the Figure 8, the array is divided into two sub-arrays arranged in a checkerboard pattern: the even array and the odd array. We then plot the distribution of the opening angle between the directions independently determined by each sub-array.

In the ALPACA collaboration, the median of this distribution is defined as the even-odd opening angle. For the current data, this value was 1.95° . Since approximately half of this value corresponds to the angular resolution, the angular resolution can be estimated to be about 1° for cosmic rays in the 5–10 TeV energy range.

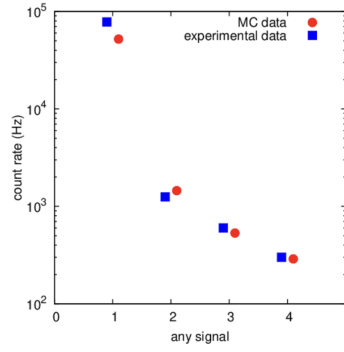


Figure 7: Comparison between the experimental and Monte Carlo data for any1 through any4 in the ALPAQUITA array. Blue squares represent the experimental data, while red circles represent the Monte Carlo simulation results.

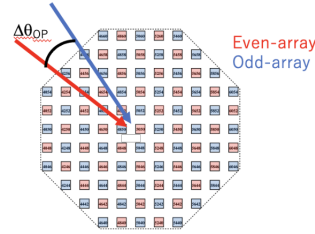


Figure 8: Explanation of even-odd opening angle. When the entire array is divided into two sub-arrays—red for the even-array and blue for the odd-array—the red vector represents the arrival direction reconstructed from the even-array, and the blue vector represents the arrival direction reconstructed from the odd-array.

5. Summary

We evaluated the detector performance by incorporating into the Monte Carlo simulation the measured characteristics of the scintillators used in the ALPAQUITA experiment—namely, the scintillation light yield, light collection time, signal rise time, and their position dependence. As a result, good agreement was observed between the experimental and simulated counting rates for any2 through any4. However, for any1, the Monte Carlo counting rate was found to be approximately 30% lower than that of the experimental data. This discrepancy is considered to arise from factors such as the zenith angle restriction in the simulation and variations in the secondary cosmic-ray intensity due to environmental changes.

Furthermore, the even-odd opening angle (an indicator of angular resolution) is well reproduced by the Monte Carlo simulation, demonstrating consistency with the observational data.

References

- [1] Kato, S. et al. , Experimental Astronomy 52, 85-107 (2021)
- [2] M.A.SubietaVasquezetal.(TheALPACA Collaboration),PoS(ICRC2023)767.

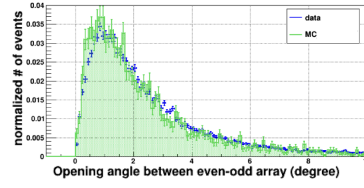


Figure 9: Comparison of the even-odd opening angle distribution between experimental data from the ALPAQUITA surface array and Monte Carlo simulations. The horizontal axis represents the even-odd opening angle, and the vertical axis shows the normalized number of events with the total normalized to unity. The blue curve corresponds to the ALPAQUITA experimental data, while the green curve represents the Monte Carlo simulation results.

- [3] The ALPACACollaboration, *Exp. Astron.* (2021) 52:85-107.
- [4] Shibata, M. et al., *ApJ* 716 1076 (2010)
- [5] D. Heck, J. Knapp, J. N. Capdevielle, G. Schatz and T. Thouw, Report FZKA, 6019, Forschungszentrum Karlsruhe (1998)
- [6] S. Agostinelli et al., *Nucl. Instrum. Methods Phys. Res., A* 506, 250 (2003)

Acknowledgements

The ALPACA project is supported by the Japan Society for the Promotion of Science (JSPS) through Grants-in-Aid for Scientific Research (B) 19H01922, Scientific Research (B) 20H01920, Scientific Research (S) 20H05640, Scientific Research (B) 20H01234, Scientific Research (B) 22H01234, Scientific Research (C) 22K03660, Scientific Research (A) 24H00220, Specially Promoted Research 22H04912 and Challenging Research (Pioneering) 24K21200, the LeoAtrox super-computer located at the facilities of the Centro de Análisis de Datos (CADS), CGSAIT, Universidad de Guadalajara, México, and by the joint research program of the Institute for Cosmic Ray Research (ICRR), The University of Tokyo. Y. Katayose is also supported by JSPS Open Partnership joint Research projects F2018, F2019. K. Kawata is supported by the Toray Science Foundation. E. de la Fuente thanks financial support from Inter-University Research Program of the Institute for Cosmic Ray Research, The University of Tokyo, grant 2023i-F-005. I. Toledano-Juarez acknowledges support from CONACyT, México; grant 754851.

Full Authors List: the ALPACA Collaboration

M. Anzorena¹, E. de la Fuente^{2,3}, K. Fujita¹, R. Garsia¹, Y. Hayashi⁴, K. Hibino⁵, N. Hotta⁶, G. Imaizumi¹, Y. Katayose⁷, C. Kato⁴, S. Kato⁸, T. Kawashima¹, K. Kawata¹, M. Kobayashi⁷, S. Kobayashi⁴, T. Koi⁹, H. Kojima¹⁰, P. Miranda¹¹, S. Mitsuishi⁴, A. Mizuno¹, K. Munakata⁴, Y. Nakamura¹, M. Nishizawa¹², Y. Noguchi⁷, S. Ogio¹, M. Ohishi¹, M. Ohnishi¹, A. Oshima^{9,13}, M. Raljevic¹¹, H. Rivera¹¹, T. Saito¹⁴, T. Sako¹, T. K. Sako¹⁵, S. Shibata¹⁰, A. Shiomi¹⁶, M. Subieta¹¹, F. Sugimoto¹, N. Tajima¹⁷, W. Takano⁵, Y. Takeyama⁷, M. Takita¹, N. Tamaki¹, Y. Tameda¹⁸, K. Tanaka¹⁹, R. Ticona¹¹, H. Tsuchiya²⁰, Y. Tsunesada^{21,22}, S. Udo⁵, G. Yamagishi⁷, Y. Yamanaka¹, K. Yamazaki⁹ and Y. Yokoe¹

¹Institute for Cosmic Ray Research, University of Tokyo, Kashiwa 277-8582, Japan.

²Departamento de Física, CUCEI, Universidad de Guadalajara, Guadalajara, México.

³Doctorado en Tecnologías de la Información, CUCEA, Universidad de Guadalajara, Zapopan, México.

⁴Department of Physics, Shinshu University, Matsumoto 390-8621, Japan.

⁵Faculty of Engineering, Kanagawa University, Yokohama 221-8686, Japan.

⁶Faculty of Education, Utsunomiya University, Utsunomiya 321-8505, Japan.

⁷Faculty of Engineering, Yokohama National University, Yokohama 240-8501, Japan.

⁸Institut d'Astrophysique de Paris, CNRS UMR 7095, Sorbonne Université, 98 bis bd Arago 75014, Paris, France,

⁹College of Science and Engineering, Chubu University, Kasugai 487-8501, Japan.

¹⁰Chubu Innovative Astronomical Observatory, Chubu University, Kasugai 487-8501, Japan.

¹¹Instituto de Investigaciones Físicas, Universidad Mayor de San Andrés, La Paz 8635, Bolivia.

¹²National Institute of Informatics, Tokyo 101-8430, Japan.

¹³College of Engineering, Chubu University, Kasugai 487-8501, Japan.

¹⁴Tokyo Metropolitan College of Industrial Technology, Tokyo 116-8523, Japan.

¹⁵Department of Information and Electronics, Nagano Prefectural Institute of Technology, Ueda 386-1211, Japan.

¹⁶College of Industrial Technology, Nihon University, Narashino 275-8575, Japan.

¹⁷RIKEN, Wako 351-0198, Japan.

¹⁸Faculty of Engineering, Osaka Electro-Communication University, Neyagawa 572-8530, Japan.

¹⁹Graduate School of Information Sciences, Hiroshima City University, Hiroshima 731-3194, Japan.

²⁰Japan Atomic Energy Agency, Tokai-mura 319-1195, Japan.

²¹Graduate School of Science, Osaka Metropolitan University, Osaka 558-8585, Japan.

²²Nambu Yoichiro Institute for Theoretical and Experimental Physics, Osaka Metropolitan University, Osaka 558-8585, Japan.